HHS Public Access

Author manuscript

Dev Dyn. Author manuscript; available in PMC 2015 May 05.

Published in final edited form as:

Dev Dyn. 2010 November ; 239(11): 3000–3012. doi:10.1002/dvdy.22437.

Dynamic Lkb1-TORC1 signaling as a possible mechanism for regulating the endoderm-intestine transition

Kathryn E. Marshall[1], **Amber J. Tomasini**[2], **Khadijah Makky**[*,2], **Suresh Kumar**[3], and **Alan N. Mayer**[1,2]

[1]Departments of Cell Biology, Neurobiology, and Anatomy, Medical College of Wisconsin, 8701 Watertown Plank Road, Milwaukee, WI 53226, USA

[2]Departments of Pediatrics, Gastroenterology Section, Medical College of Wisconsin, 8701 Watertown Plank Road, Milwaukee, WI 53226, USA

[3]Department of Pathology, Medical College of Wisconsin, 8701 Watertown Plank Road, Milwaukee, WI 53226, USA

Summary

The intestinal epithelium arises from undifferentiated endoderm via a developmental program known as the endoderm-intestine transition (EIT). Previously we found that the target of rapamycin complex 1 (TORC1) regulates intestinal growth and differentiation during the EIT in zebrafish. Here we address a possible role for the tumor suppressor kinase Lkb1 in regulating TORC1 in this context. We find that TORC1 activity is transiently upregulated during the EIT in both zebrafish and mouse. Concomitantly, Lkb1 becomes transiently localized to the nucleus, suggesting that these two phenomena may be linked. Morpholino-mediated knockdown of *lkb1* stimulated intestinal growth via upregulation of TORC1, and also induced precocious intestine-specific gene expression in the zebrafish gut epithelium. Knockdown of *tsc2*, which acts downstream of *lkb1*, likewise induced early expression of intestine-specific genes. These data suggest that programmed localization of Lkb1 could represent a novel mechanism for regulating the EIT during intestinal development in vertebrates.

Keywords

Lkb1; intestine; zebrafish; endoderm-intestine transition; organogenesis; morphogenesis; differentiation

Introduction

In vertebrates, the intestine forms via a conserved sequence of developmental events. The first developmental intermediate is the primitive gut tube. It is fashioned from the endoderm by folding in mammals and birds (Montagne et al., 1999) or canalization in teleosts (Ng et

Corresponding author and address: Alan N. Mayer, Department of Pediatrics, astroenterology Section, Medical College of Wisconsin, 8701 Watertown Plank Road, Milwaukee, WI 53226, Phone: 414-456-5894, Fax: 414-456-6632, alanmayer@mac.com.

*Current address: Department of Biomedical Sciences, College of Health Sciences, Marquette University, Schroeder Complex 426, P.O. Box 1881, Milwaukee, WI 53201, khadijah.makky@marquette.edu

al., 2005). Mature intestinal architecture then emerges through a complex series of events collectively known as the endoderm-intestine transition (EIT). The EIT features multiple cellular processes - morphogenesis, proliferation, and differentiation- acting in concert to yield a single-layered absorptive epithelium (Trier and Moxey, 1979). In mammals, the primitive gut endoderm is a multilayered (stratified) epithelium, but then adopts a single layered configuration by forming secondary lumina (Trier and Moxey, 1979). In contrast, in teleosts (i.e. zebrafish), the primitive gut endoderm remains a single-layered (simple) epithelium throughout the EIT (Trotter et al., 2009). In both cases, an anterior-posterior wave of tissue remodeling, proliferation and cell differentiation leads to formation of intestinal villi. The mechanisms that control this complex event remain poorly defined.

The target of rapamycin (TOR) pathway regulates tissue growth across eukaryotic species (Wullschleger et al., 2006). TOR, the kinase for which the pathway is named, is stimulated by growth factors and nutrients, and is inhibited in their absence. In the context of a developing or regenerating organ, TOR activity is required for activating anabolic pathways required for cell growth and proliferation (Hwang et al., 2008). Although TOR is expressed ubiquitously, its activity can be subject to regulation by tissue-specific and developmental factors (Hwang et al., 2008). For example, recently we showed that the rapamycin-sensitive TOR complex 1 (TORC1) is required for the EIT in zebrafish (Makky et al., 2007). Inhibition of TORC1 by pharmacologic and genetic manipulation leads to arrest of intestinal growth, morphogenesis, and intestine-specific gene expression. Other studies on the role of TORC1 in the intestine have shown a role for cell migration in the adult intestine (Rhoads et al., 2006), suggesting a shared requirement for TORC1 in tissue development and repair.

To investigate how TORC1 may be regulated during intestinal development, we focused on an upstream regulator, the serine/threonine kinase, Lkb1. Lkb1 represses TORC1 signaling and inhibits downstream processes such as protein biosynthesis and cell cycle progression (Corradetti et al., 2004; Shaw et al., 2004). Lkb1 also modulates cell polarity via targets separate from the TOR pathway (Mirouse et al., 2007; Amin et al., 2009). Lkb1 kinase activity is regulated by subcellular localization via binding to its two cofactors, Strad and MO25 (Boudeau et al., 2003; Hawley et al., 2003). When complexed with its binding partners, Lkb1 localizes to the cytoplasm and kinase activity is stimulated over 10-fold (Baas et al., 2003; Boudeau et al., 2003). The human polyposis syndrome Peutz-Jeghers can result from mutations in Lkb1 that disrupt either its catalytic activity or, more commonly, its ability to form a productive ternary complex with Strad and MO25 (Zeqiraj et al., 2009).

The role of Lkb1 during intestinal development has not yet been directly examined. Homozygous genetic ablation of *LKB1* in mice results in embryonic lethality due to vascular defects prior to development of most organ systems (Ylikorkala et al., 2001; Jishage et al., 2002). In contrast, the heterozygous mutant recapitulates many of the features of Peutz-Jeghers Syndrome. Tissue-specific null mutations of *LKB1* have also been reported, including pancreas- (Hezel et al., 2008), intestinal mesenchyme- (Katajisto et al., 2008), and intestinal epithelial-specific knockouts (Shorning et al., 2009). In the latter study, the intestinal epithelial-specific gene deletion was induced postnatally, resulting in a defect in secretory lineages. In the present study, we addressed the question of how Lkb1 might

regulate TOR signaling during intestinal development in the zebrafish and mouse. The results described below suggest a novel mechanism by which Lkb1 may control the EIT.

Results

TORC1 activity is transiently upregulated in the developing intestinal epithelium

To monitor the temporal regulation of TORC1 during development, we used the phosphorylated form of ribosomal protein S6 (RPS6) by immunofluorescence. In the zebrafish, we found that phospho-RPS6$_{ser240/244}$ was transiently upregulated in the gut epithelium, peaking around 72 hpf (Fig. 1). Interestingly, the peak of fluorescence intensity corresponds to the timing of rapamycin-induced arrest of intestinal development (Makky and Mayer, 2007; Makky et al., 2007). The staining pattern is heterogeneous, suggesting significant cell-cell variability in the amount of TORC1 activity present in each cell. To verify that the immunofluorescence was a specific readout of TORC1 activity, we pretreated embryos with rapamycin at 48 hpf, and this resulted in complete loss of the fluorescence signal at 72 hpf (Fig. 1B). Histometric analysis showed that the aggregate fluorescence intensity increased progressively from 48 to 72 hpf, then dropped down to baseline by 96 hpf, consistent with transient upregulation of TORC1 during the EIT (Fig. 1C).

We also performed immunostaining for phospho-RPS6$_{ser240/244}$ in embryonic mouse intestine across the analogous stages of intestinal development (e13.5-15.5, Fig. 2). The staining pattern in the mouse was similar to the zebrafish, increasing transiently at e14.5, which represents the midpoint and most dynamic phase of the EIT. We quantified this observation by measuring mean fluorescence intensity within the epithelium. On a 0-4095 gray-scale, mean intensities roughly doubled from e13.5 to 14.5, then declined to baseline at 15.5. Each interval change showed statistical significance ($P<0.05$). Thus, TORC1 activity appears to be subject to developmental regulation in the endoderm during vertebrate intestinal morphogenesis.

Zebrafish Lkb1: sequence conservation and gene expression

A possible source of developmental regulation for TORC1 is the serine-threonine kinase, Lkb1. We identified the zebrafish ortholog of Lkb1 using the mouse and human LKB1 proteins to query the NCBI sequence database. We identified a full length cDNA (GenBank accession no. **BC092776**) encoding a protein with 78% identity to the mouse LKB1 and 80% identity to human LKB1 (Supplementary Fig. 1). Homology search against the assembled zebrafish genome (Zv8) yielded only one locus on Chromosome 6 encoding a protein with high homology to Lkb1 orthologs (GenBank accession no. **NC_007117**). Other related proteins with less than 35% identity aligned mostly in the canonical kinase domain. These data suggest a single locus in the zebrafish genome encodes an Lkb1 ortholog.

We performed *in situ* hybridization to monitor *lkb1* gene expression during the period of intestinal morphogenesis from 24-120 hpf (Fig. 3). *Lkb1* expression occurs at all larval stages and is widely distributed. Expression is present in the digestive organs, with higher expression in the midgut relative to the fore-or hindgut.

Lkb1 displays dynamic subcellular localization during the EIT

As a readout of Lkb1 activity, we monitored its subcellular localization during development (Boudeau et al., 2003). When bound to its binding partners, Lkb1 localizes to the cytoplasm and kinase activity increases. Conversely, Lkb1 variants that are localized constitutively to the nucleus lack kinase activity. Due to technical difficulties with antibody staining of zebrafish tissue, we monitored Lkb1 localization using a transgenic line expressing Lkb1-mCherry fusion protein under control of the globally active β-actin promoter [β-actin:Lkb1-mcherry] (Lkb1-mCh). Previous studies have shown that C-terminal fluorescent protein fusions to Lkb1 do not perturb subcellular localization or biological activity (Baas et al., 2004). The transgenic fish appear morphologically normal and are not discernibly different from wild-type siblings. At 48 hpf in the primitive gut tube, Lkb1-mCherry localized mostly to the cytoplasm of intestinal epithelial cells (Fig. 4). Then, between 48 and 72 hpf, the protein became localized mostly to the nucleus. After 77 hpf, as the epithelium began to adopt a more columnar morphology, nuclear localization became less distinct. Then at 96 hpf after the intestinal epithelium adopted a differentiated morphology, Lkb1-mCh was seen mostly in the cytoplasm.

We also monitored Lkb1 immunofluorescence in the mouse embryonic intestinal epithelium at stages e13.5, e14.5 and e15.5, corresponding to the pre-, mid- and post-EIT epithelium, respectively. To track this morphogenic progression, we co-stained for f-actin which marks the apices of polarized epithelial cells. The results show a biphasic pattern analogous to that seen in the zebrafish. Lkb1 was about equally distributed in nucleus and cytoplasm at e13.5 with a nuclear/cytoplasmic ratio 1.14±0.4 (n=6 sections). At e14.5, the midpoint of the EIT is marked by the formation of secondary lumina. During this stage, Lkb1 redistributes toward the nucleus as reflected by an increased nuclear/cytoplasmic of 2.09±0.76 (n=9 sections) (e13.5 vs e14.5, $p<0.01$). At e15.5, the epithelium adopts a single-layered architecture and a simple columnar morphology, and Lkb1 staining redistributes back to the cytoplasm with a nuclear/cytoplasmic ratio of 1.13±0.49 (n=4, e14.5 vs e15.5, $p<0.05$).

Nuclear localization of Lkb1 corresponds with upregulation of TORC1

When comparing the timing of upregulation of TORC1 (Fig. 1) with that of Lkb1 nuclear localization (Fig. 4), there appears to be a temporal overlap between these phenomena, suggesting they may be linked. To test this more directly, we performed immunostaining for phospho-$RPS6_{ser240/244}$ in Lkb1-mCh fish (Fig. 6). On the whole, the timing of upregulation of phospho-$RPS6_{ser240/244}$ corresponded temporally with the nuclear localization of Lkb1-mCh in the gut epithelium. There were single cells that were pRPS6-negative/nuclear Lkb1-mCh, and pRPS6-positive/cytoplasmic Lkb1-mCh, but these were in the minority. These data suggest that the transient upregulation of TORC1 in the gut epithelium during the EIT might result, at least in part, from the nuclear localization of Lkb1.

Considering both the zebrafish and mouse data, these results represent the first example, to our knowledge, in which Lkb1 localization changes predictably within a defined developmental program. As discussed below, transient nuclear localization of Lkb1 could thus represent a mechanism for modulating TORC1 activity during epithelial growth and morphogenesis.

Knockdown of lkb1 in zebrafish

Since the nuclear localization of Lkb1 likely results in downregulation of the kinase, we sought to mimic this effect using morpholino-mediated knockdown. We generated and characterized two non-overlapping morpholinos to target either an internal splice junction (spl MO) in the kinase domain or the translation start site (ATG MO) (Supplementary Fig. 2). Western blotting using an antibody to human LKB1 revealed a band at the expected molecular weight of about 50 kD that was absent in the morpholino-injected embryos ("morphants"). A five base pair mismatch (5 mm MO) and a random 25-mer (25 N MO) morpholino did not affect Lkb1 protein expression. We also noted a morpholino-insensitive band at approximately 46 kD, which may represent a cross-reacting kinase since the antibody was made to an epitope in the highly conserved serine/threonine kinase domain (Supplementary Fig. 2B). We also monitored knockdown at the mRNA level by RT-PCR. The spl MO induced knockdown of the *lkb1* transcript at 72 hpf, with no effect on 5 mm MO- or 25 N MO-injected embryos (Supplementary Fig. 2A). As a functional readout for the efficacy of the morpholinos, we monitored phosphorylation of RPS6 $_{ser240/244}$ by western blot (Supplementary Fig. 2C). This showed induction of phospho-RPS6$_{ser240/244}$, consistent with the activation of TORC1 in the morphants.

Knockdown of lkb1 results in a larger intestine

Interestingly, the *lkb1* morphant embryos appeared normal by live stereomicroscopy (Supplementary Fig. 3). However, upon histological sectioning, we noted that the intestine was larger in the morphants compared to controls (Fig. 7A). Morphometric analysis of *lkb1* morphant intestine revealed an 18% to 42% increase in numbers of intestinal epithelial cells per cross section (n=25 embryos per treatment, $p<0.05$; Fig. 7B). Cell morphology also was affected, with about 20% increased height-to-width ratio of the epithelial cells at 96 hpf, indicating that the morphant cells were more columnar in shape (Fig. 7B). In addition, there appears to be a more prominent brush border, suggestive of increased apical specialization in the *lkb1* morphant, which may reflect more advanced differentiation.

To account for increased cell number, we determined if cell proliferation was increased in the *lkb1* morphants by measuring the rate of BrdU incorporation (Fig. 7C). At 48 hpf, the fraction of BrdU-positive epithelial cells was 48% higher in the spl morphant compared to the uninjected control (n=25 embryos per treatment, $p<0.005$). Similarly, at 72 hpf, the morphant intestine contained 41% more BrdU-positive cells compared to the uninjected (n=25 embryos per treatment $p<0.05$). In contrast, at 96 hpf the BrdU incorporation rate showed a 30% decrease in BrdU staining relative to control (n=25 embryos per treatment, $p<0.005$). This might be explained by alterations in developmental timing, as discussed below.

Lkb1 is an upstream regulator of TORC1, but acts through many other targets as well. To test whether the effects of Lkb1 knockdown result from TORC1 activation, we analyzed the effect of *lkb1* KD in the presence of rapamycin. Treatment with rapamycin alone resulted in a previously observed phenotype, in which the gut remains small and poorly differentiated. However, *lkb1* knockdown did not lead to any incremental enlargement of the gut,

suggesting that rapamycin can block this phenotype (Fig. 8). This is consistent with TORC1 acting downstream of *lkb1* to regulate intestinal growth.

Knockdown of Lkb1 promotes earlier intestinal differentiation

The EIT is a complex developmental process involving both tissue growth, morphogenesis and cell differentiation. As yet, it is not known if these processes are linked by a common upstream regulator. Based on the data we presented above, we hypothesized that Lkb1 could modulate the timing of cell differentiation as well as tissue growth. Accordingly, we analyzed expression of intestine-specific markers in the *lkb1* morphants. Typically, enterocyte-specific gene expression begins at about from 72 hpf in the most anterior portion of the gut, and proceeds posteriorly (Wallace et al., 2005). However, we noted that at 48 hpf, by *in situ* hybridization, expression of *intestinal fatty acid binding protein* (*ifabp*) (Mudumana et al., 2004) was higher in the *lkb1* morphants (Fig. 9A). To better quantify this effect we performed quantitative RT-PCR for several enterocyte-specific genes (Fig. 9B). At 48 and 72 hpf, *ifabp* showed upregulated expression in the morphants (between 33-37% increase, respectively; $p<0.05$;). *Intestinal alkaline phosphatase* (*iap*) levels (Bates et al., 2007) increased by 50% in both morphants compared to the uninjected control ($p<0.05$). The ileal-specific *sodium/bile-acid co-transporter* (*slc10a2)*, a relatively later marker, increased between 29-42% in the morphants ($p<0.05$). Thus *lkb1* knockdown appears to induce precocious onset of differentiation. One alternative explanation includes the possibility that increased transcript reflects a proportionate enlargement of the intestine. But at 48 hpf, the morphants contain the same number or fewer intestinal cells than the controls (see Fig. 7). Also, Lkb1 might be inducing higher baseline gene expression levels, but at later time points there were no significant differences in *ifabp* or *iap* expression between controls and morphants (not shown).

We also analyzed the timing of goblet cell differentiation in the *lkb1* morphant using wheat germ agglutinin (WGA) to stain for goblet cell mucin (Wallace et al., 2005). Using this marker, we show that *lkb1* knockdown promoted earlier goblet cell differentiation in the hindgut at 96 hpf (Fig. 9C). By 121 hpf, goblet cell populations were comparable, indicating that the effect is not likely to be a reflection of altered lineage allocation. Taken together with the gene expression studies, we view these data as supporting a role for Lkb1 in regulating the timing of the intestinal differentiation program.

To rule out the possibility that *lkb1* knockdown stimulates global acceleration of development, as an internal control we examined both lateral line migration (not shown) and the timing of retinal lamination, which occurs contemporaneously with the EIT (Supplementary Fig. 4). Between 24 hpf and 96 hpf, only slight differences between morphants and controls were noted, with morphant eyes appearing less well developed compared to control. Based on these readouts, a global acceleration of development seems unlikely to account for our observations on the timing of intestinal development.

Upregulation of TORC1 induces intestinal differentiation

Lkb1 is known to modulate the AMPK-TSC2-TOR cascade (Corradetti et al., 2004). To further address if this pathway mediates the effects of *lkb1* knockdown on intestinal

development, we tested whether activating TORC1 downstream of Lkb1 would produce a similar phenotype. To accomplish this, we performed morpholino-mediated knockdown of the *tsc2* gene (Fig. 10). The *tsc2* spl MO induced knockdown of the *tsc2* message and generated a larger splice variant detected by RT-PCR (Fig. 10A). We also show that *tsc2* knockdown upregulated phospho-RPS6$_{ser240/244}$, reflecting the activation of TORC1 (Fig. 10B). Quantitative RT-PCR of intestinal markers shows upregulated early expression in the *tsc2* morphant. We detected upregulation of *ifabp* and *iap* at 48 hpf (56% and 400% increase; $p<0.005$). At 72 hpf, there was a non- significant increase in *ifabp* (37% $p>0.05$), but *iap* was significantly higher (47% increase; $p<0.05$). At 96 hpf, *slc10a2* expression was 228% higher than in uninjected controls ($p<0.05$; Fig. 10C). These data, showing earlier expression of intestinal markers in the *tsc2* morphants, are consistent with the notion that TORC1 can regulate the timing of intestinal differentiation during the EIT.

Discussion

The developmental regulation of the EIT remains poorly understood, despite its detailed description decades ago (Coulombre and Coulombre, 1958; Trier and Moxey, 1979; Chalmers and Slack, 1998; Wallace et al., 2005). A promising approach to identifying genes required for the EIT has been classical genetic analysis using the zebrafish (Allende et al., 1996; Mayer and Fishman, 2003; Amsterdam et al., 2004; Yee et al., 2007; Davuluri et al., 2008; de Jong-Curtain et al., 2009). The zebrafish has distinct advantages in that morphogenesis can be quickly scored in the live embryo, and the cellular architecture of the intestine is simpler compared with mammals. However, one pitfall of this approach may be that the genes implicated are required for downstream cellular processes such as ribosome biogenesis, RNA processing and transport, and protein biosynthesis, rather than serving in regulatory roles (Allende et al., 1996; Pack et al., 1996; Mayer and Fishman, 2003; Amsterdam et al., 2004; Yee et al., 2007; Davuluri et al., 2008; de Jong-Curtain et al., 2009). Nonetheless, these cited studies offer a hint that the EIT might be regulated by a common upstream pathway that controls anabolic growth, such as TOR kinase (Hwang et al., 2008).

Recently, we demonstrated that TORC1 exerts permissive control over the EIT in zebrafish (Makky et al., 2007). Here, we provide evidence suggesting that TOR pathway signaling may function instructively as well, to regulate the timing and duration of the EIT. This idea is supported by the observation that phosphorylation of RPS6 is transiently increased in the intestinal epithelium during the EIT, and that forced activation of TORC1 leads to precocious development. To evaluate a possible source of developmental regulation for TORC1, we studied the potential role of Lkb1 kinase. We found that, in both zebrafish and mouse, Lkb1 localizes transiently to the nucleus during the midpoint of the EIT. Prior studies have shown that Lkb1 kinase activity can be regulated by subcellular localization, supporting the idea that intestinal growth during the EIT may be regulated by this mechanism. The intestine thus offers the first known example, to our knowledge, of the developmental regulation of Lkb1 via its nuclear-cytoplasmic localization.

It is well established that Lkb1 activity increases when Lkb1 is localized to the cytoplasm. In fact, translocation of Lkb1 to the cytoplasm is sufficient to polarize single intestinal epithelial cells (Baas et al., 2004). In contrast, nuclear localization results in downregulation

of Lkb1 kinase activity with consequent TORC1 activation, leading to increased cell proliferation (Shaw et al., 2004). In this study we showed that Lkb1 is localized to the nucleus during the TORC1-dependent phase of cell proliferation in the intestinal epithelium. After an interval that may be regulated by the intestine's developmental program, translocation of Lkb1 to the cytoplasm then corresponds with the observed decreased in cell proliferation. In this context, knockdown of Lkb1 may mimic the programmed nuclear localization of Lkb1, thereby initiating the EIT precociously, and possibly prolonging the interval during which TORC1 is activated. This would lead to a larger intestine, which we observed in the *lkb1* morphants.

Taken together, these observations suggest a hypothetical model for the regulation of the EIT by TORC1, as modulated by the nuclear/cytoplasmic translocation of Lkb1 (Fig. 11). Developmental signals that control progression from endoderm to intestine could act in part via Lkb1 localization resulting in the upregulation of TORC1, and triggering the intestine's growth and differentiation program through numerous downstream mediators yet to be identified. A subsequent signal (or possibly loss of the initial signal) would then induce Lkb1 translocation to the cytoplasm, leading to the downregulation of TORC1. Although cell morphogenesis was not specifically addressed in this work, this model would also be compatible with the role of Lkb1 in regulating cell polarity through pathways distinct from TORC1 (ten Klooster et al., 2009). In addition, there are many other upstream inputs that control TORC1 activity that could act independently or in concert with Lkb1.

The upstream mechanisms that regulate Lkb1 localization are still poorly defined, but likely involve modulation of binding to partners Strad and MO25. The mechanisms by which these interactions are modulated during the EIT are yet to be discovered, but may involve regulation of the ternary complex that allosterically activates Lkb1 (Zeqiraj et al., 2009). Recently, the histone deacetylase SIRT1 was shown to activate Lkb1 by promoting its association with Strad and localization to the cytoplasm (Lan et al., 2008). Since SIRT1 activity is dependent on cellular redox status (NAD+/NADH), this protein or another NAD +-dependent deacetylase could transmit cellular energy status to Lkb1 and regulate intestinal growth in response to nutrient availability (Tou et al., 2004). Other potential mechanisms for regulating Lkb1 localization include post-translational modulation of Strad, MO25, or the cellular import/export machinery (Dorfman and Macara, 2008). Temporal control of Lkb1 localization could thus represent a novel developmental mechanism for controlling transitions between primitive and differentiated tissues. The EIT offers a well-defined developmental context to dissect this mechanism further.

Experimental Procedures

Fish stocks and embryo culture—The TuAB line was used to generate wild-type embryos. Zebrafish were maintained and mated as described previously (Westerfield, 1995). Embryos were either collected and raised at 28.4°C, or embryos were delayed in development by rearing them at 25°C for the first 24 hpf and then shifting the embryos to 28.4°C. If embryos were delayed, the developmental stage will be noted with an asterisk. Live images were captured using a Leica MZFLIII dissecting microscope.

Tg[β-actin:Lkb1-mCherry] transgenic zebrafish

We employed the Tol2 kit (Kwan et al., 2007) to generate the β-actin:Lkb1-mCherry construct. BP reactions used the full- length *lkb1* minus the stop codon to insert *lkb1* into the P4-P1R vector to create a middle-entry clone. Then, the LR reaction combined the *β-actin* promoter 5′-entry clone, *lkb1* middle-entry clone, and the *mCherry* 3′-entry clone into the destination vector #394 containing Tol2 transposon sites. The DNA construct (35 pg/nl) and Tol2 transposase RNA (50 pg/nl) were coinjected into the one-cell stage embryo. At 24 hpf, embryos were selected for red fluorescence and grown to adulthood. Starting at three months of age, the male G0 fish were out-crossed to WT TuAB fish to establish lines. Red F1 positive embryos from the resulting out-crossings were reared to adulthood and each fish was established as a unique line.

Imaging Lkb1-mCherry in the zebrafish intestine—Red F1 and F2 positive embryos were fixed in 2% PFA for 2 hours at room temperature, cryoprotected through a sucrose gradient, and embedded in OCT. Embryos were cryosectioned at 12 μm thick sections and counterstained with DAPI to label nuclei. See Imaging and Processing for detailed description of obtaining immunofluorescent images.

RNA *in situ* hybridization—Probe synthesis and whole-mount RNA *in situ* hybridization were performed as described previously (Mayer and Fishman, 2003). After probe synthesis, the resulting reaction was spun through an Illustra ProbeQuant™ G-50 Micro Column (GE Healthcare) to purify the RNA probe. Gene-specific forward and reverse primers are as listed: *lkb1*: F5′ gag gat gag gag gag gat gaa gag-3′, R5′-ttt aca taa gac ccc tcg cc-3′; *ifabp*: F5′-gcc cat gac aac ctg aag at-3′, R5′-ttt gac att ggg agt gca ga-3′. Reverse primers were synthesized with a T7 polymerase recognition sequence (5′-taa tac gac tca cta tag gg -3′) on the 5′ tail of the primer.

Rapamycin treatment—Embryos were dechorionated and treated with 400 nM rapamycin in the embryo media beginning at 24 hpf and refreshed daily as described previously (Makky and Mayer, 2007).

Morpholino knockdown—Morpholinos were obtained from Gene Tools. They were diluted into Danieau's solution and injected into the 1-cell stage embryo in concentrations ranging between 200-300 μM as indicated. *Lkb1* morpholino antisense oligonucleotides were designed corresponding to the second exon-intron junction (spl MO- ata agc atc agc tcc tac ttc ttg) and the start site (ATG MO-gcc cac gct cat ctt tat tat aaa c) of the *lkb1* zebrafish genomic sequence. Splicing interference was detected by RT-PCR across the targeted exon using the following primers: F5′-cat ctg gac tac ctg acg gag aac-3′, R5′- ttt gtg gac gat tcc ctg gct gtg-3′. In addition, a five base pair mismatch (5 mm MO- ata aac cat cac gtc gta ctt gtt g) and a mixture of 25-mer morpholino sequences (25 N MO) were designed to control for morpholino toxicity and backbone side effects. For *tsc2* knockdown (cDNA Genbank accession #**XM_690820**, genomic accession #**NC_007112**), the splice MO was designed to span an exon-intron junction of the *tsc2* gene (*tsc2* spl MO: 5′- aac agt gtt att tac cgt ctg cga g-3′) and splicing interference was detected by RT-PCR across the targeted exon.

Quantitative RT-PCR—Total RNA was extracted from 10 embryos at various time points using Trizol (Invitrogen) according to manufacturer's protocol. Reverse transcription was performed using oligo (dT)20 primers and SuperScript™ II reverse transcriptase. cDNA was used for either PCR reactions using Taq (Qiagen) or qRT-PCR reactions using QuantiTect™ SYBR® Green PCR kit (Qiagen). Primer pairs are intestine-specific *alkaline phosphatase*: F5′-atg gga gtg tcc acg gtt tca-3′, R5′- cga tgc caa cag act ttc ctt g-3′; *ef1α*: F5′-ctt ctc agg ctg act gtg c-3′, R5′-ccg cta gca tac cct cc-3′; *ifabp*: F5′-gcc cat gac aac ctg aag at-3′, R5′-ttt gac att ggg agt gca ga-3′; *slc10a2*: F5′- tgt ttt ctg cta ctg gct tga tgg-3′, R5′-atg agg acg att ccc acc aca g-3′. qRT-PCR samples were run in triplicate and normalized to a standard curve for *ef1α* transcript levels for each cDNA.

Immunological and histological techniques

Histological methods—For histology, zebrafish embryos were processed and sectioned as in Makky et al. (2007). The pancreatic islet and size of the neural tube were used as anatomical landmarks for anterior-posterior position. Morphometric analysis was performed as in Makky et al. (2007) for cell number, and height-to-width ratio. Counts were obtained from 20-25 embryos spanning three different injection experiments. The mean and standard deviation for measurements collected from control and morpholino-injected embryos were graphed and statistical analysis was performed using a two-tailed t-test (Microsoft Excel).

Zebrafish Immunofluorescence—Zebrafish larvae at various stages were fixed in Dent's fixative (20% DMSO/80% methanol) for 2 h to overnight. Embryos were rehydrated into PBT (PBS + 0.1% Tween-20) and blocked for 1 h at room temperature in blocking buffer (5% Normal Goat Serum, 1% BSA, 0.1% Tween-20 in PBS). Embryos were incubated in primary antibodies in blocking buffer overnight at 4°C, then washed with PBT 4 times for 10 min each and incubated with goat secondary antibody conjugated to Alexafluor® 546 (red) or Alexafluor® 488 (green) overnight at 4°C. After extensive washing with PBT, embryos were dehydrated in an ethanol/water gradient then embedded into JB4 (Polysciences, Inc.). Four μm-thick sections were generated and counterstained with DAPI. Immunofluorescence was imaged using a motorized Zeiss Axioplan microscope. Images were captured using a Q-imaging digital camera and OpenLab 4.0.2 (Improvision). Z-stacks were deconvolved using Volocity 3.1 (Improvision), then processed for figures using Adobe Photoshop CS2. In cases where brightness or contrast adjustment was needed to convey the findings, both controls and experimental samples were adjusted in parallel. Mean fluorescence intensity was measured using Openlab (Imrpovision). Intestines from six sections were outlined and analyzed by the “measure” tool. The average of all intensities was normalized to the mean intensity.

Mouse LKB1 Immunofluorescence—Mouse embryos were collected at various stages, guts dissected out and fixed in 4% PFA for 2 hours at 4°C. Specimens were cryoprotected through a sucrose gradient and embedded in OCT. Frozen blocks were sectioned in 10 μm-thick increments. Sections were permeablized in PBS containing 3% Triton X-100, blocked with PBT containing 1% BSA/5% sheep serum, and then incubated overnight in a humid chamber in primary antibody. Sections were then washed in PBT and incubated for 1 h at room temperature with the secondary antibody in a humid chamber, washed, and

counterstained with DAPI. Primary antibodies used for immunofluorescence were as follows: Na+/K+ ATPase (α5, 1:25, Developmental Studies Hybridoma Bank); phospho-RPS6$_{ser240/244}$, 1:500, Cell Signaling Technology #2215); Lkb1 (1:100, abcam #ab58786). Confocal microscopy (LSM510, Zeiss) images (512×512 or 1024×1024 pixels, averaged twice) were acquired using LSM510 software v.3.2 in the multitrack mode and 63×, 1.2 NA water immersion lens. The field of view varied between 71- 202 micron and the zoom was either 0.7 for stage 14 and 15 or 1 for stage 12-13. The pixel saturation was corrected using grey scale images and software assisted PMT gain/offset correction. The A548 signal was collected in channel 1 (LP575, excited with Diode 561 nm - AOTF set at 14%) and DAPI signal was collected in channel 2 (BP420-480, excited with 405 nm - AOTF set at 5%). Additional A488 signal was collected in channel 3 (BP505-550, excited with multi line argon laser 488 nm - AOTF set at 5%). The merged images were used for protein localization analysis using the colocalization module of the LSM510 software to track the changes in red pixel staining intensity in the nucleus. We first defined the threshold for channel 1 to capture all staining above background, then classified localization as nuclear or cytoplasmic depending on overlap with DAPI staining. The field of analysis was marked using phalloidin labeling to define the epithelium. The aggregate amount of Lkb1 represented by channel 1 was calculated by multiplying number of pixels analyzed within the given compartment (nuclear or nonnuclear) by intensity per pixel.

Goblet cell staining—Goblet cell mucin was detected by rhodamine-conjugated wheat germ agglutinin (1:100 dilution in PBT, Vector Laboratories) as in (Makky and Mayer, 2007). Proteinase K concentration used was 70μg/ml for 35 min at 28.4°C.

BrdU staining—Uninjected and morphant embryos were processed and stained for BrdU cell labeling as described previously (Makky and Mayer, 2007).

Western blotting—Embryos were collected at 48 or 72 hpf and homogenized in SDS lysis buffer (50 mM Tris-HCl (pH 7.6), 50 mM NaCl, 1 mM EDTA, 1% Triton X100, 0.1% SDS, 1 tablet of Complete Mini, EDTA-free protease inhibitor cocktail (Roche Diagnostics) in water). Homogenates were sonicated 2 × 30 seconds, spun down at 13,200 × g for 15 min at 4°C, and the supernatant was collected and stored at –80°C. Supernatant samples (5 μg) were resolved by 10% SDS-PAGE and analyzed by Western blot. The following antibodies were used: Lkb (1:1000, abcam #ab58786); phospho- RPS6$_{ser240/244}$, 1:500, Cell Signaling Technology #2215); total RPS6 (1:2000, Cell Signaling Technologies #2317); α-tubulin (1:1000, Sigma #T6199).

Statistical analysis—All statistics were performed using Excel (unpaired, two-tailed student's t-test). Samples were determined to be statistically significant if the p-value was less than or equal to 0.05.

Supplementary Material

Refer to Web version on PubMed Central for supplementary material.

Acknowledgments

Funding for this work was provided in part from the Digestive Disease Center of the Medical College of Wisconsin, NIH/NIDDK (R21-DK073468), Advancing a Healthier Wisconsin, and the Children's Research Institute. We thank Drs. Ramani Ramchandran and Brian Link for their critical reading of the manuscript. We thank members of the Link lab for assistance with zebrafish transgenesis. We appreciate the valuable assistance of Drs. Kathy Shim and Jian Zhang for help with obtaining staged embryonic mouse intestine. All animal work was performed in accordance with institutional guidelines under the auspices of protocols approved by the IACUC.

References

Allende ML, Amsterdam A, Becker T, Kawakami K, Gaiano N, Hopkins N. Insertional mutagenesis in zebrafish identifies two novel genes, pescadillo and dead eye, essential for embryonic development. Genes Dev. 1996; 10:3141–3155. [PubMed: 8985183]

Amin N, Khan A, St Johnston D, Tomlinson I, Martin S, Brenman J, McNeill H. LKB1 regulates polarity remodeling and adherens junction formation in the Drosophila eye. Proc Natl Acad Sci U S A. 2009; 106:8941–8946. [PubMed: 19443685]

Amsterdam A, Nissen RM, Sun Z, Swindell EC, Farrington S, Hopkins N. Identification of 315 genes essential for early zebrafish development. Proc Natl Acad Sci U S A. 2004; 101:12792–12797. [PubMed: 15256591]

Baas AF, Boudeau J, Sapkota GP, Smit L, Medema R, Morrice NA, Alessi DR, Clevers HC. Activation of the tumour suppressor kinase LKB1 by the STE20-like pseudokinase STRAD. Embo J. 2003; 22:3062–3072. [PubMed: 12805220]

Baas AF, Kuipers J, van der Wel NN, Batlle E, Koerten HK, Peters PJ, Clevers HC. Complete polarization of single intestinal epithelial cells upon activation of LKB1 by STRAD. Cell. 2004; 116:457–466. [PubMed: 15016379]

Bates JM, Akerlund J, Mittge E, Guillemin K. Intestinal alkaline phosphatase detoxifies lipopolysaccharide and prevents inflammation in zebrafish in response to the gut microbiota. Cell Host Microbe. 2007; 2:371–382. [PubMed: 18078689]

Boudeau J, Baas AF, Deak M, Morrice NA, Kieloch A, Schutkowski M, Prescott AR, Clevers HC, Alessi DR. MO25alpha/beta interact with STRADalpha/beta enhancing their ability to bind, activate and localize LKB1 in the cytoplasm. Embo J. 2003; 22:5102–5114. [PubMed: 14517248]

Chalmers AD, Slack JM. Development of the gut in Xenopus laevis. Dev Dyn. 1998; 212:509–521. [PubMed: 9707324]

Corradetti MN, Inoki K, Bardeesy N, DePinho RA, Guan KL. Regulation of the TSC pathway by LKB1: evidence of a molecular link between tuberous sclerosis complex and Peutz-Jeghers syndrome. Genes Dev. 2004; 18:1533–1538. [PubMed: 15231735]

Coulombre AJ, Coulombre JL. Intestinal development. I. Morphogenesis of the villi and musculature. J Embryol Exp Morphol. 1958; 6:403–411. [PubMed: 13575653]

Davuluri G, Gong W, Yusuff S, Lorent K, Muthumani M, Dolan AC, Pack M. Mutation of the zebrafish nucleoporin elys sensitizes tissue progenitors to replication stress. PLoS Genet. 2008; 4:e1000240. [PubMed: 18974873]

de Jong-Curtain TA, Parslow AC, Trotter AJ, Hall NE, Verkade H, Tabone T, Christie EL, Crowhurst MO, Layton JE, Shepherd IT, Nixon SJ, Parton RG, Zon LI, Stainier DY, Lieschke GJ, Heath JK. Abnormal nuclear pore formation triggers apoptosis in the intestinal epithelium of elys-deficient zebrafish. Gastroenterology. 2009; 136:902–911. [PubMed: 19073184]

Dorfman J, Macara IG. STRADalpha regulates LKB1 localization by blocking access to importin-alpha, and by association with Crm1 and exportin-7. Mol Biol Cell. 2008; 19:1614–1626. [PubMed: 18256292]

Fishman MC. Zebrafish--the canonical vertebrate. Science. 2001; 294:1290–1291. [PubMed: 11701913]

Hawley SA, Boudeau J, Reid JL, Mustard KJ, Udd L, Makela TP, Alessi DR, Hardie DG. Complexes between the LKB1 tumor suppressor, STRAD alpha/beta and MO25 alpha/beta are upstream kinases in the AMP-activated protein kinase cascade. J Biol. 2003; 2:28. [PubMed: 14511394]

Hezel AF, Gurumurthy S, Granot Z, Swisa A, Chu GC, Bailey G, Dor Y, Bardeesy N, Depinho RA. Pancreatic LKB1 deletion leads to acinar polarity defects and cystic neoplasms. Mol Cell Biol. 2008; 28:2414–2425. [PubMed: 18227155]

Hwang M, Perez CA, Moretti L, Lu B. The mTOR signaling network: insights from its role during embryonic development. Curr Med Chem. 2008; 15:1192–1208. [PubMed: 18473813]

Jishage K, Nezu J, Kawase Y, Iwata T, Watanabe M, Miyoshi A, Ose A, Habu K, Kake T, Kamada N, Ueda O, Kinoshita M, Jenne DE, Shimane M, Suzuki H. Role of Lkb1, the causative gene of Peutz-Jegher's syndrome, in embryogenesis and polyposis. Proc Natl Acad Sci U S A. 2002; 99:8903–8908. [PubMed: 12060709]

Katajisto P, Vaahtomeri K, Ekman N, Ventela E, Ristimaki A, Bardeesy N, Feil R, DePinho RA, Makela TP. LKB1 signaling in mesenchymal cells required for suppression of gastrointestinal polyposis. Nat Genet. 2008; 40:455–459. [PubMed: 18311138]

Kwan KM, Fujimoto E, Grabher C, Mangum BD, Hardy ME, Campbell DS, Parant JM, Yost HJ, Kanki JP, Chien CB. The Tol2kit: a multisite gateway-based construction kit for Tol2 transposon transgenesis constructs. Dev Dyn. 2007; 236:3088–3099. [PubMed: 17937395]

Lan F, Cacicedo JM, Ruderman N, Ido Y. SIRT1 modulation of the acetylation status, cytosolic localization, and activity of LKB1. Possible role in AMP-activated protein kinase activation. J Biol Chem. 2008; 283:27628–27635. [PubMed: 18687677]

Makky K, Mayer AN. Zebrafish Offers New Perspective on Developmental Role of TOR Signaling. Organogenesis. 2007; 3:67–69. [PubMed: 19279702]

Makky K, Tekiela J, Mayer AN. Target of rapamycin (TOR) signaling controls epithelial morphogenesis in the vertebrate intestine. Dev Biol. 2007; 303:501–513. [PubMed: 17222402]

Mayer AN, Fishman MC. Nil per os encodes a conserved RNA recognition motif protein required for morphogenesis and cytodifferentiation of digestive organs in zebrafish. Development. 2003; 130:3917–3928. [PubMed: 12874115]

Mirouse V, Swick LL, Kazgan N, St Johnston D, Brenman JE. LKB1 and AMPK maintain epithelial cell polarity under energetic stress. J Cell Biol. 2007; 177:387–392. [PubMed: 17470638]

Montagne J, Stewart MJ, Stocker H, Hafen E, Kozma SC, Thomas G. Drosophila S6 kinase: a regulator of cell size. Science. 1999; 285:2126–2129. [PubMed: 10497130]

Mudumana SP, Wan H, Singh M, Korzh V, Gong Z. Expression analyses of zebrafish transferrin, ifabp, and elastaseB mRNAs as differentiation markers for the three major endodermal organs: liver, intestine, and exocrine pancreas. Dev Dyn. 2004; 230:165–173. [PubMed: 15108321]

Ng AN, de Jong-Curtain TA, Mawdsley DJ, White SJ, Shin J, Appel B, Dong PD, Stainier DY, Heath JK. Formation of the digestive system in zebrafish: III. Intestinal epithelium morphogenesis. Dev Biol. 2005; 286:114–135. [PubMed: 16125164]

Pack M, Solnica-Krezel L, Malicki J, Neuhauss SCF, Schier AF, Stemple DL, Driever W, Fishman MC. Mutations affecting development of zebrafish digestive organs. Development. 1996; 123:321–328. [PubMed: 9007252]

Rhoads JM, Niu X, Odle J, Graves LM. Role of mTOR signaling in intestinal cell migration. Am J Physiol Gastrointest Liver Physiol. 2006; 291:G510–517. [PubMed: 16710051]

Shaw RJ, Bardeesy N, Manning BD, Lopez L, Kosmatka M, DePinho RA, Cantley LC. The LKB1 tumor suppressor negatively regulates mTOR signaling. Cancer Cell. 2004; 6:91–99. [PubMed: 15261145]

Shorning BY, Zabkiewicz J, McCarthy A, Pearson HB, Winton DJ, Sansom OJ, Ashworth A, Clarke AR. Lkb1 deficiency alters goblet and paneth cell differentiation in the small intestine. PLoS ONE. 2009; 4:e4264. [PubMed: 19165340]

ten Klooster JP, Jansen M, Yuan J, Oorschot V, Begthel H, Di Giacomo V, Colland F, de Koning J, Maurice MM, Hornbeck P, Clevers H. Mst4 and Ezrin induce brush borders downstream of the Lkb1/Strad/Mo25 polarization complex. Dev Cell. 2009; 16:551–562. [PubMed: 19386264]

Tou L, Liu Q, Shivdasani RA. Regulation of mammalian epithelial differentiation and intestine development by class I histone deacetylases. Mol Cell Biol. 2004; 24:3132–3139. [PubMed: 15060137]

Trier JS, Moxey PC. Morphogenesis of the small intestine during fetal development. Ciba Found Symp. 1979:3–29. [PubMed: 261525]

Trotter AJ, Parslow AC, Heath JK. Morphologic analysis of the zebrafish digestive system. Methods Mol Biol. 2009; 546:289–315. [PubMed: 19378111]

Wallace KN, Akhter S, Smith EM, Lorent K, Pack M. Intestinal growth and differentiation in zebrafish. Mech Dev. 2005; 122:157–173. [PubMed: 15652704]

Westerfield, M. The Zebrafish Book. The University of Oregon Press; Eugene: 1995.

Wullschleger S, Loewith R, Hall MN. TOR signaling in growth and metabolism. Cell. 2006; 124:471–484. [PubMed: 16469695]

Yee NS, Gong W, Huang Y, Lorent K, Dolan AC, Maraia RJ, Pack M. Mutation of RNA Pol III subunit rpc2/polr3b Leads to Deficiency of Subunit Rpc11 and disrupts zebrafish digestive development. PLoS Biol. 2007; 5:e312. [PubMed: 18044988]

Ylikorkala A, Rossi DJ, Korsisaari N, Luukko K, Alitalo K, Henkemeyer M, Makela TP. Vascular abnormalities and deregulation of VEGF in Lkb1-deficient mice. Science. 2001; 293:1323–1326. [PubMed: 11509733]

Zeqiraj E, Filippi BM, Deak M, Alessi DR, van Aalten DM. Structure of the LKB1-STRAD-MO25 Complex Reveals an Allosteric Mechanism of Kinase Activation. Science. 2009

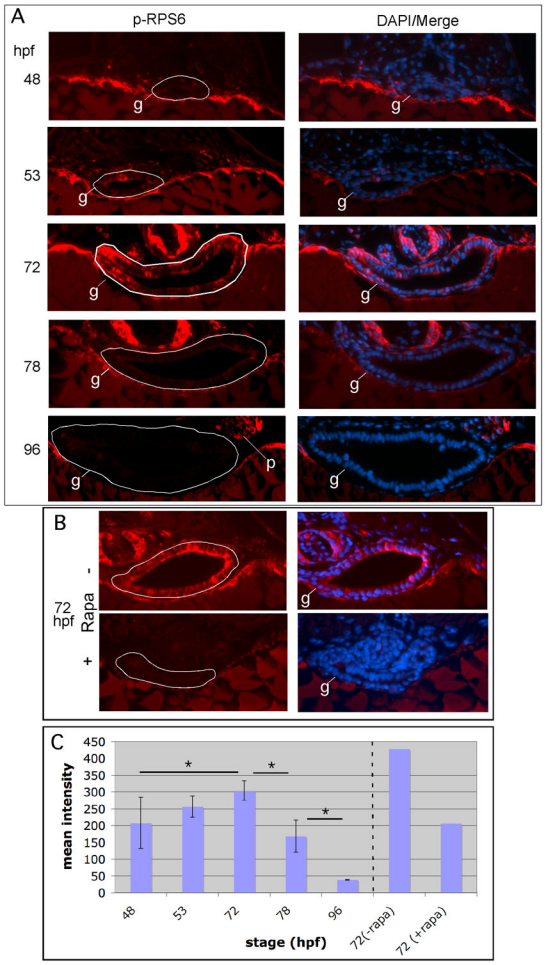

Figure 1. TORC1 is transiently upregulated during the EIT in zebrafish

(A) Zebrafish embryos were stained via whole mount immunofluorescence for P-RPS6$_{ser240/244}$, followed by sectioning in JB-4 and counterstaining with DAPI. The white line delineates the gut epithelium (g). The number of immunopositive cells and staining increases from 48 to 72 hpf, then decreases upon cytodifferentiation of the epithelium. (B) To verify that the fluorescent signal is a specific readout of TORC1, we treated embryos with 100 μM rapamycin for 24 hours prior to fixation. This resulted in significant reduction of the immunofluorescence signal. (C) Mean fluorescence intensity (grayscale 0-4095) of the epithelium immunostained for P-RPS6$_{ser240/244}$. Sections shown in panel A, as well as additional representative sections (total n=4 for each stage) were subjected to histometric analysis using the program Openlab to calculate the mean fluorescence intensity for the intestinal epithelium. For panel B, only the sections shown were subjected to analysis. P-values less than 0.05 are indicated by an asterisk.

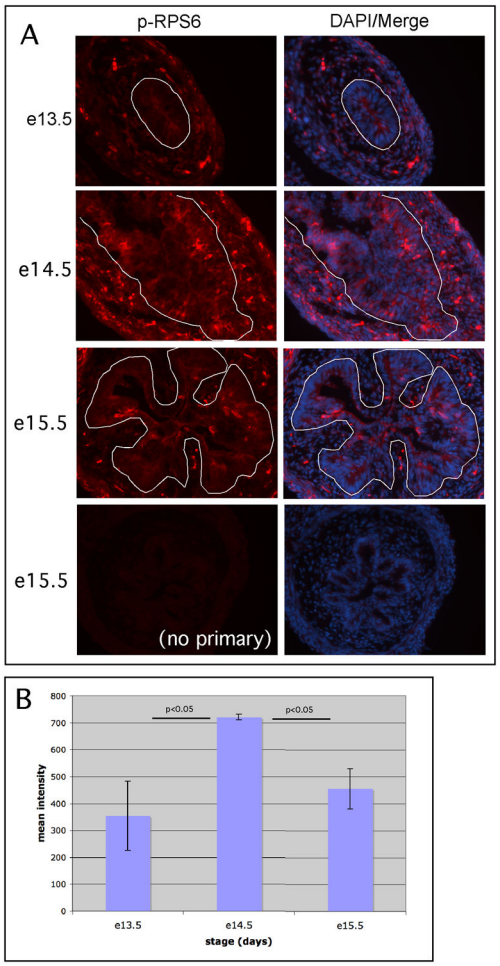

Figure 2. TORC1 is transiently upregulated during the EIT in the mouse embryonic intestine

(A) Sections of embryonic mouse intestine were stained for P-RPS6$_{ser240/244}$ and then counterstained with DAPI. Weak immunostaining is seen at e13.5 (pre-EIT), with marked increase in number and intensity of immunopositive cells at e14.5 (mid-EIT). At e15.5, shortly after the formation of a simple columnar epithelium, a few residual epithelial cells remain positive, but the signal is substantially decreased compared with e15.5. The white line delineates the epithelium from subjacent mesenchyme. (B) Quantification of fluorescence intensity in the epithelium shows a pattern in which mean intensity peaks at e14.5. Shown are representatives of n=4 sections from each stage that were analyzed. T-test showed significant differences ($p<0.05$) between e13.5 *vs* 14.5, and e14.5 *vs* 15.5).

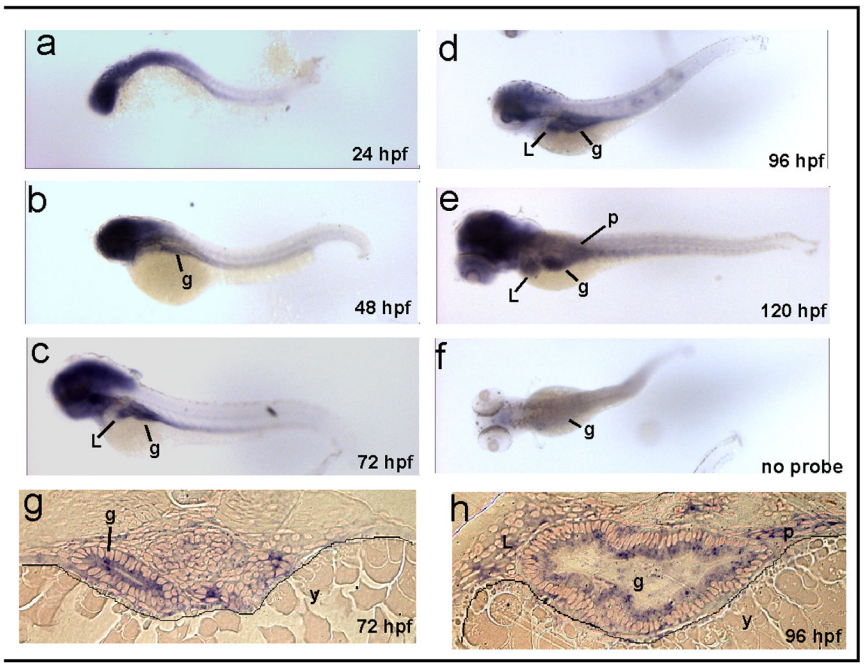

Figure 3. Zebrafish *lkb1* is widely expressed

a-f: Whole-mount *in situ* hybridization to zebrafish *lkb1* shown in dorso-lateral view with the head to the left. Background staining was determined by omitting the RNA probe in panel f. g and h: Histological sections of embryos in panels c and d, respectively. Solid lines delineate gut tube from the yolk. Original magnification: a-f, 40×; g and h, 400×. Abbreviations: g, gut; L, liver; p, pancreas; y, yolk.

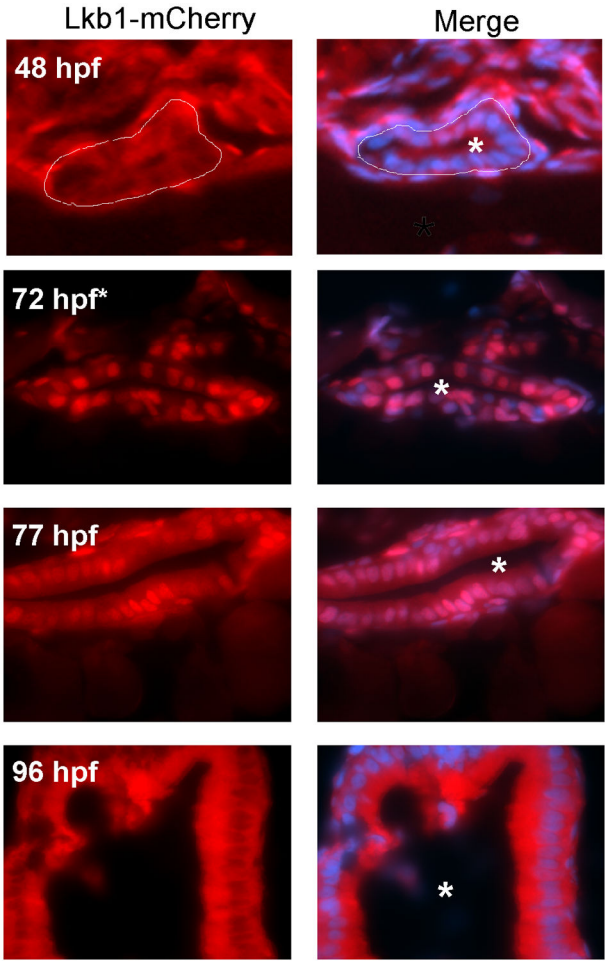

Figure 4 . Lkb1 displays dynamic subcellular localization during the EIT in zebrafish

(A) Lkb1 subcellular localization was monitored in a Tg[β-*actin: lkb1- mCherry*] zebrafish line at 48 hpf, 72 hpf*, 77 hpf, and 96 hpf. Frozen sections were counterstained with DAPI (blue). A white line outlines the gut tube at 48 hpf, and asterisks mark the gut lumen. Original magnification: 630×.

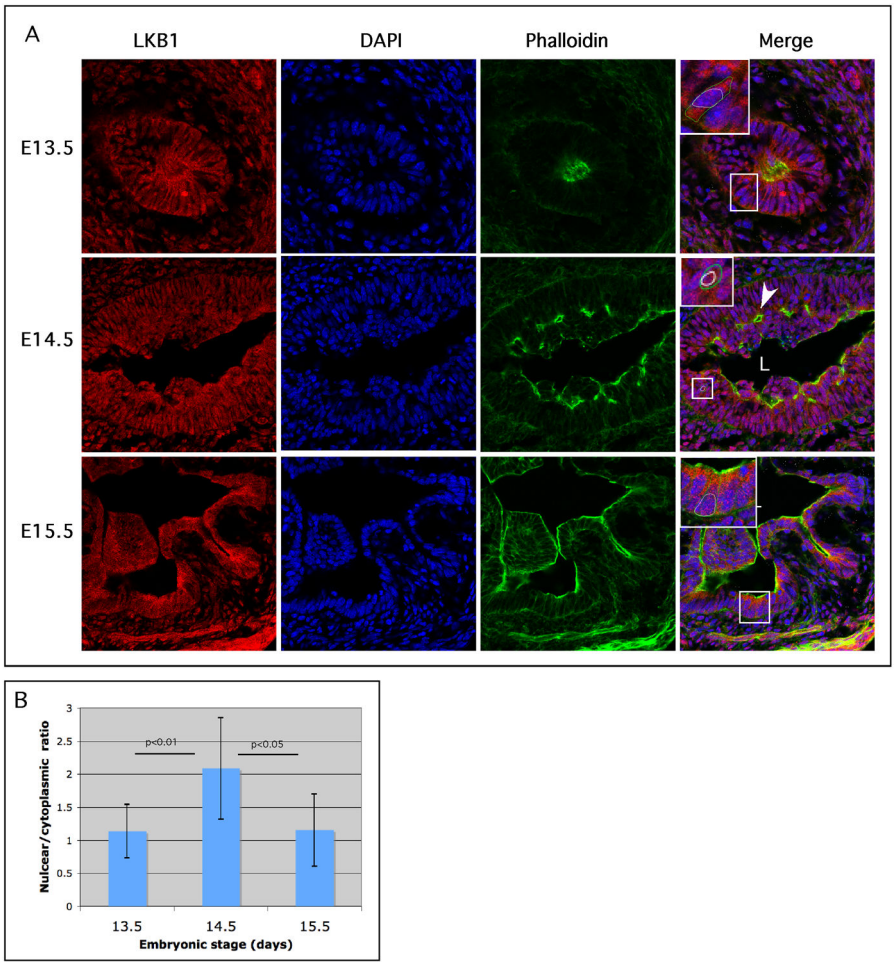

Figure 5. Lkb1 displays dynamic subcellular localization during the EIT in embryonic mouse intestine

(A) Confocal images of Lkb1 (red) counterstained with phalloidin (green) to reveal cell apices and DAPI (blue) to mark nuclei. Lkb1 becomes increasingly localized to nuclei as the EIT proceeds from primitive gut tube (e13.5) to transitional epithelium. At e14.5, a secondary lumen within the epithelium is marked by phalloidin (arrowhead). Upon formation of a simple columnar epithelium at 15.5, staining in the nuclei is relatively decreased, though still present. Original magnification, 630×. Insets in merged images show 3× digital magnification of area outlined by boxes, with a single cell boundary and nucleus outlined by green and white, respectively. (B) Histometric analysis of Lkb1 staining intensity within the epithelium reveals dynamic distribution of Lkb1 in nuclear and non-nuclear (i.e. cytoplasmic) cellular compartments during the EIT.

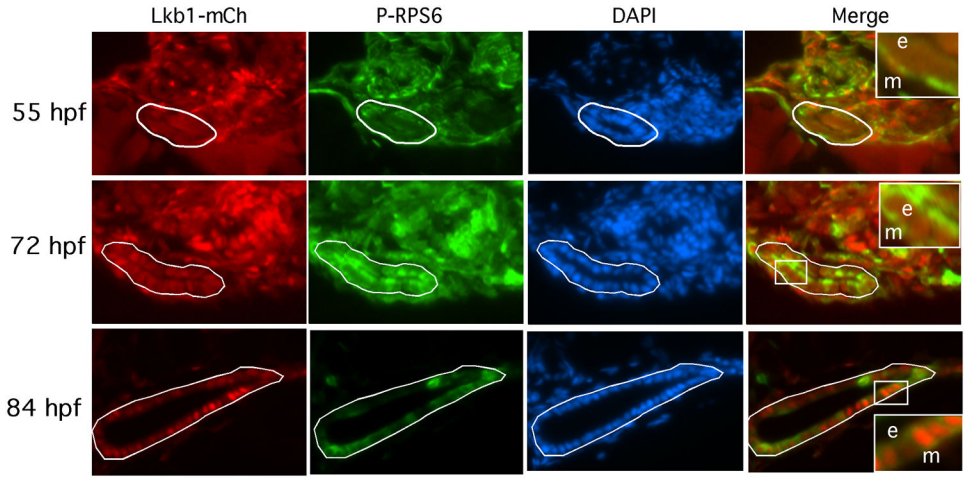

Figure 6. Co-imaging of Lkb1 localization and TORC1 activation

Zebrafish expressing Lkb1-mCherry (red) at the indicated stages were immunostained for P-RPS6$_{ser240/244}$ (green). The stages shown represent pre-, mid-, and early post-EIT. At **55 hpf,** Lkb1 is diffusely present in the scant cytoplasm of intestinal epithelial cells, though it can be seen in the nuclei of various other cell types outside the intestine. Staining for P-RPS6$_{ser240/244}$ is low relative to surrounding tissue. At **72 hpf,** Lkb1-mCherry is seen in the nuclei of most of the intestinal epithelial cells, and P-RPS6$_{ser240/244}$ immunostaining is increased relative to 55 hpf. At **84 hpf**, nuclear localization of Lkb1-mCherry is sporadically seen in the epithelium, and most (though not all) of those cells stain positive for P-RPS6$_{ser240/244}$. A white line encloses the gut epithelium. Original magnification, 200×. Insets, 600×. e, epithelium; m, mesenchyme.

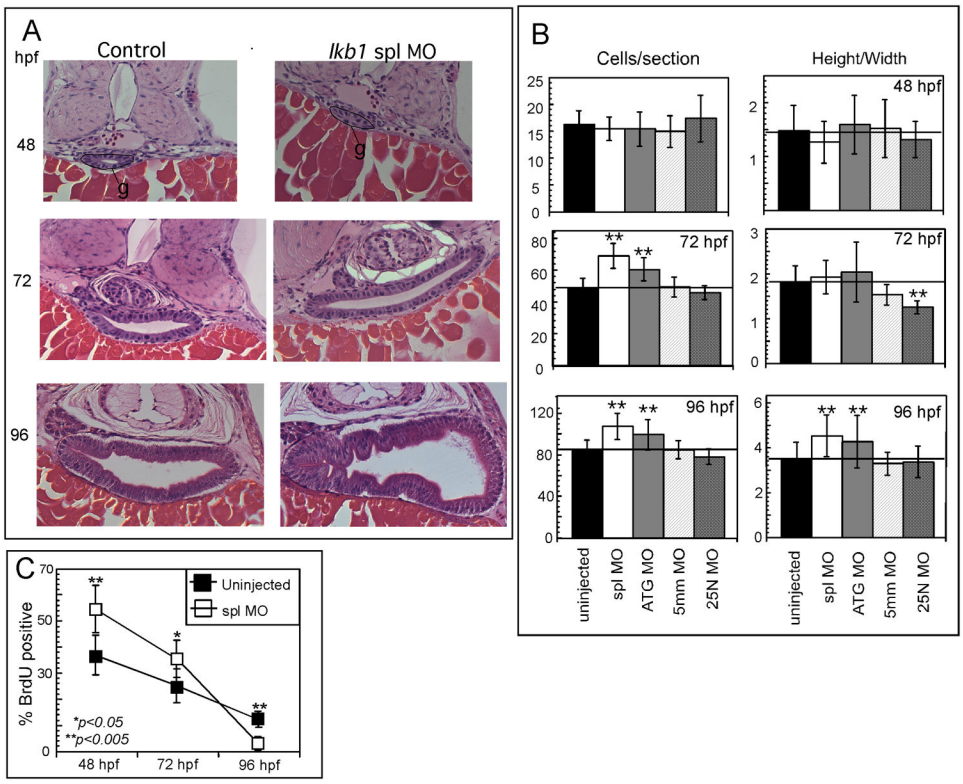

Figure 7. Knockdown of *lkb1* stimulates epithelial cell proliferation and growth

(A) Histological sections through the intestine of uninjected, spl morphant, and ATG morphant, embryos at 48 hpf, 72 hpf, and 96 hpf. At 48 hpf the gut lumen is outlined by solid black line. g, gut. Shown are representative sections that correspond to the median gut size as determined by morphometry and depicted in the bar graph. Sections were stained with H&E and original magnification was 400×. (B) Depiction of morphometric analysis for cell number and cell shape (height-to-width ratio) using 25 embryos per treatment. A-P positions were matched between embryos using standard anatomic landmarks (pancreatic islet, gall bladder, neural tube). (C) Analysis of proliferation rate by BrdU incorporation comparing uninjected (black squares) and spl morphant (white squares) at 48, 72, and 96 hpf. Significance was determined using Student's two-tail, unpaired t-test (n=25 embryos). Single asterisk, $p<0.05$; double asterisk, $p<0.005$.

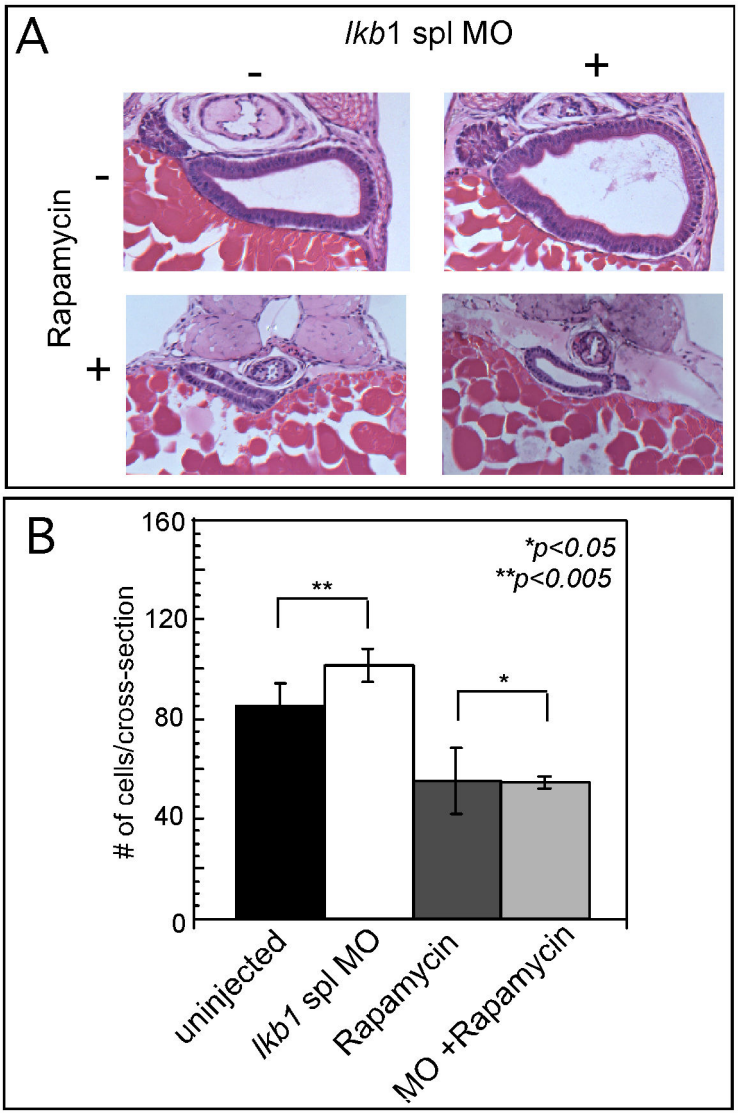

Figure 8. *Lkb1* regulates intestine size via TORC1

(A) Histological analysis of intestine at 96 hpf in *lkb1* spl morphants in the presence and absence of rapamycin. Sections were stained with H&E. Original magnification: 400×. (B) Morphometric analysis of cell number showing no morphant phenotype in the presence of rapamycin (n=6 embryos).

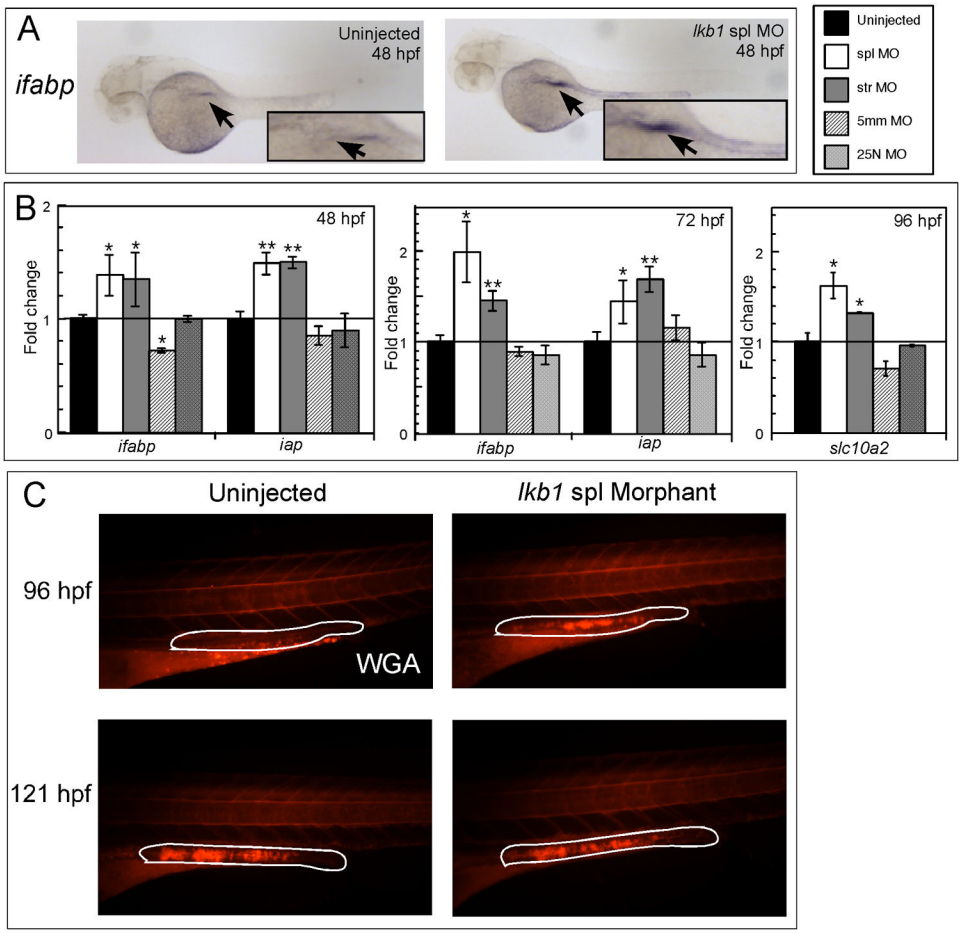

Figure 9. Knockdown of *lkb1* induces precocious expression of intestinal markers

(A) *In situ* hybridization to *intestinal fatty acid binding protein (ifabp)* at 48 hpf. Arrow indicates the gut tube, showing increased expression in the *lkb1* morphant. Original magnification, 40×. (B) Relative mRNA expression of intestinal markers *ifabp* and *iap* at 48 hpf and 72 hpf, and *slc10a2* at 96 hpf in uninjected, spl, ATG, 5 mm, and 25 N determined by qRT-PCR. Samples were run in triplicate and normalized to *ef1α* to control for total RNA. Significance was determined using Student's two-tail, unpaired t-test. (C) Rhodamine-conjugated wheat germ agglutinin (WGA) staining for goblet cells in the uninjected and *lkb1* spl morphant at 96 hpf and 121 hpf. Very few goblet cells are visible in the control embryo, whereas the morphant displays a much brighter signal. At 121 hpf, the fluorescent signals are qualitatively similar between control and morphant. White line encircles the hindgut. Original magnification: 40×.

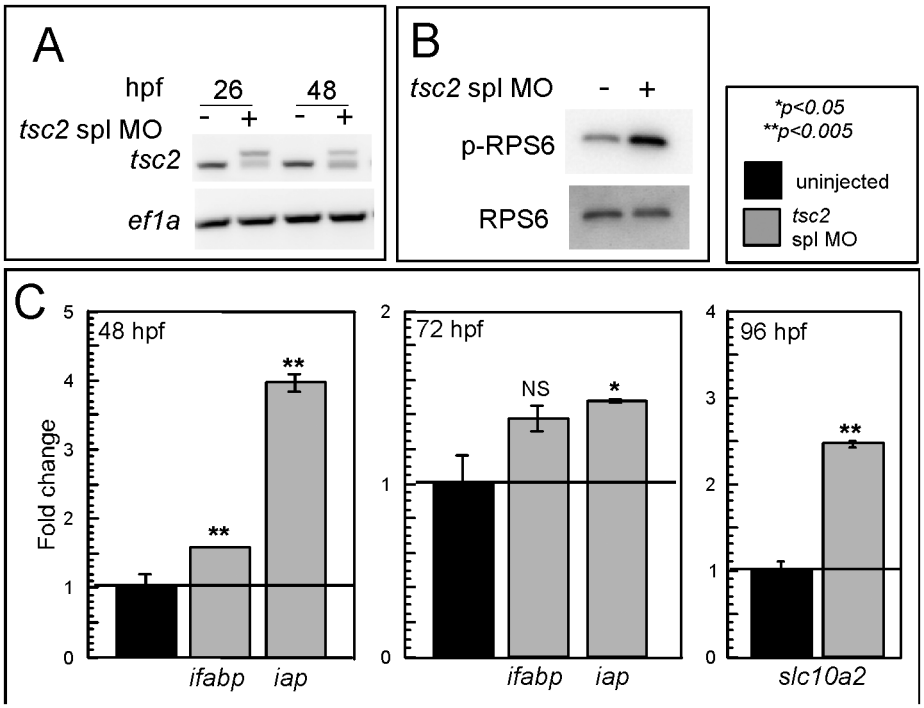

Figure 10. *Tsc2* knockdown induces precocious expression of intestinal markers

(A) RT-PCR demonstrating knockdown of *tsc2* in spl MO-injected embryos. (B) Western blot of extract from *tsc2* spl morphants at 53 hpf for P-RPS6$_{ser240/244}$, showing upregulation of TORC1 signaling. (C) qRT-PCR of *tsc2* morphant RNA for markers of intestinal differentiation showing upregulation of *ifabp* and *iap* expression at 48 hpf and 72 hpf, and *slc10a2* at 96 hpf. Samples were normalized to *ef1α* and significance was determined using Student's two-tail, unpaired t-test.

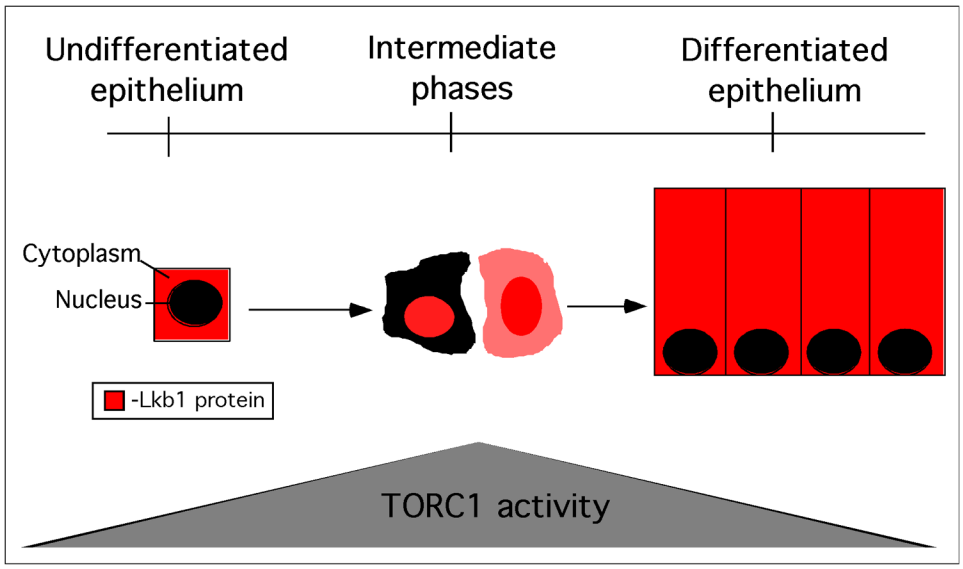

Figure 11. Suggested model for the role of Lkb1 in regulating the EIT

We hypothesize that the EIT requires the formation of a developmental intermediate characterized by the transient relocalization of Lkb1 from the cytoplasm to the nucleus. Consequently, TORC1 becomes upregulated, promoting epithelial growth and differentiation. After the intestine reaches a target size, Lkb1 then relocalizes to the cytoplasm, TOR activity decreases, and the cells become stabilized in a terminally differentiated state. The source and identity of the signals regulating Lkb1 in this context remain to be identified.